JOURNAL OF GEOPHYSICAL RESEARCH, VOL. 103, NO. A7, PAGES 14,979–14,986, JULY 1, 1998

Constraints on Jovian plasma properties from a dispersion analysis of unducted whistlers in the warm Io torus

K. Wang[1] and R. M. Thorne

Department of Atmospheric Sciences, University of California, Los Angeles

R. B. Horne

British Antarctic Survey, Natural Environment Research Council, Cambridge, England

W. S. Kurth

Department of Physics and Astronomy, University of Iowa, Iowa City

Abstract. The dispersion of unducted lightning-generated whistlers observed by Voyager 1 in the warm torus around density peaks at $L = 5.7$ and $L = 5.9$ are analyzed using the HOTRAY code, which incorporates a newly developed diffusive equilibrium density model for the Io torus. Since the wave propagation characteristics are primarily controlled by electron density, a simplified two-ion (H^+ and O^+) model has been used to simulate wave dispersion. The properties of O^+ are adjusted to simulate the electron density variation at low latitudes ($\leq 20°$), where heavy ions dominate, and a variable H^+ component is added to model the electron density at higher latitudes. Both the offset and tilt of the Jovian magnetic dipole are taken into account to determine the electron distribution as a function of System III longitude. The results confirm earlier suggestions that modest therml anisotropies ($T_\perp > T_\parallel$) of heavy ions are required to match the observed whistler dispersion. Proton concentrations typically lie in the range 5-10%, with larger values in the outer torus. On the basis of these optimum plasma parameters, the observed upper cutoff frequencies ($\sim$ 6 kHz) imply a minimum electron density of about 8 cm^{-3} at high latitudes along field lines that map into the warm torus. This analysis of unducted whistlers indicates that all observed waves originate in the northern hemisphere rather than the southern hemisphere, as assumed in earlier studies of ducted waves. This new result is consistent with optical lightning events, which were only observed in the northern hemisphere by Voyager 1.

1. Introduction

Lightning-generated whistlers were detected by the plasma wave instrument on Voyager 1 in three distinct regions near the inner edge of the Io torus [*Gurnett et al.*, 1979; *Gurnett and Scarf*, 1983; *Kurth et al.*, 1985]. The initial dispersion analyses of these waves indicated that lightning in the Jovian atmosphere was the most likely source [*Gurnett et al.*, 1979]. A new three-dimensional model for the distribution of plasma in the inner Jovian magnetosphere has been developed, and the model parameters have been optimized using the constraints imposed by a detailed analysis of the dispersion and spectral properties of whistlers in the warm torus.

The dispersion of whistlers was initially used as a remote probe for plasma properties in the Earth's inner magnetosphere [*Helliwell*, 1965; *Smith and Angerami*, 1968]. Subsequently, the dispersion of Jovian whistlers was analyzed to estimate the electron and light ion (H^+) densities along field-aligned propagation paths between the Jovian ionosphere and the Io torus [*Tokar et al.*, 1982a, b]. Furthermore, under the assumptions that the observed upper cutoff frequency is equal to the minimum plasma frequency (which is valid when waves propagate strictly along the field direction), *Gurnett et al.* [1981] obtained an estimate of 1 cm^{-3} for the minimum density along the ray path. The thermal proton concentration, which could not be detected directly by the Voyager PLS (plasma science) instrument, was

[1]Now at Jet Propulsion Laboratory, Pasadena, California.

Paper number 98JA00964.
0148-0227/98/98JA-00964$09.00

also estimated to be around 1 to 10% near the equator based on the assumption that waves propagate along field lines [*Tokar et al.*, 1982a, b].

In the earlier studies, density models were simplified either by assuming an exponential distribution of plasma density along field lines [*Gurnett et al.*, 1981; *Tokar et al.*, 1982a] or by assuming a diffusive equilibrium distribution in which the magnetic mirror force due to ion temperature anisotropies was neglected [*Tokar et al.*, 1982b]. Nevertheless, temperature anisotropies (with $T_{\perp} > T_{\parallel}$) are expected since heavy ions in the torus are produced by a pickup process. Subsequently, the diffusive equilibrium density model was extended to include the effects of temperature anisotropies of plasma species [*Huang and Birmingham*, 1992], and detailed Io torus plasma profiles were modeled based on both Voyager 1 PLS data and UVS (ultraviolet spectrometer) compositional information [*Bagenal*, 1994]. *Crary et al.* [1996] applied this improved model to reanalyze whistler dispersions in the Io torus assuming field-aligned propagation and concluded that thermal ion anisotropies were required to best account for the observed whistler dispersion. Furthermore, the proton abundance was found to be $\leq$10% which was lower than the results of earlier whistler analyses [*Tokar et al.*, 1982a, b], primarily due to the revised ion temperatures [*Bagenal et al.*, 1985].

The plasma model developed by *Crary et al.* [1996] indicates a minimum plasma frequency near 20 kHz at high latitudes along field lines that map into the Io torus. For strictly field aligned propagation, this implies that waves below 20 kHz could, in principle, have access to the Io torus. However, the observed upper cutoff frequency is typically near 6 kHz, and, based on detailed ray tracing, *Wang et al.* [1995] have shown that Jovian whistlers do not necessarily propagate along the field direction. Instead, waves from a broad range of latitudes in the ionosphere can be guided to the observation location by the density maxima of the Io torus. In addition, there is substantial variability in both the whistler dispersion and the upper cutoff frequency for waves observed at essentially the same regions in the Io torus [*Kurth et al.*, 1985], implying that the whistlers did not follow the same propagation paths and must be unducted [*Wang et al.*, 1995]. For oblique wave propagation, the assumption that the observed upper cutoff frequency is equal to the minimum local plasma frequency is no longer valid; the upper cutoff frequency for observed whistlers can be substantially lower than the minimum local plasma frequency along the propagation paths of waves. An earlier study of unducted whistler propagation [*Wang et al.* 1995] also indicated that the lightning source location was at lower latitudes ($L \leq 4$, $\lambda_{m,0} \leq 60°$). The waves could thus avoid propagation through the high electron density regions at high latitudes of the Io torus.

To date, the observed upper cutoff frequencies have not been adequately explained and the source location of these whistlers has been derived from density models which assume a centered dipole magnetic field [*Mei et al.*, 1995; *Wang et al.*, 1995]. In order to accurately analyze observed whistler dispersion and the wave spectral properties, a comprehensive three-dimensional (3-D) analytical density model has been developed which accounts for longitudinal variations of the centrifugal equator as well as the temperature anisotropies of the plasma. A realistic model for the inner plasmaspheric density has also been incorporated based on a detailed analysis of whistler observations in the cold Io torus [*Wang et al.*, this issue]

2. Models and Dispersion Analysis With HOTRAY

The Jovian magnetic field is assumed to be dipolar with an offset and tilt given by the OTD (offset and tilt of the dipole) model in *Acuña et al.* [1983]. Three distinct plasma density models are used to represent the ionosphere, the inner plasmasphere, and the Io torus: (1) The ionospheric profile is an empirical fit to the Voyager data [*Strobel and Atreya*, 1983] and is composed simply of electrons and H^+. The peak density is comparable to 10^5 cm^{-3} at 1.02 R_J, with an exponential scale height of 1000 km at higher altitude [*Wang et al.*, 1995]. (2) The inner plasmasphere model (also composed of H^+ and electrons) is a modified empirical fit to the Pioneer 10 and 11 data, adapted from the earlier model of *Sentman and Goertz* [1978] and *Divine and Garrett* [1983]. (3) Plasma components of the Io torus are based on the analytical model of *Mei et al.* [1995]. The temperature of each component is assumed to be constant along any field line, but realistic variations in L value [*Bagenal*, 1994] are included. The offset and tilt of the dipole are taken into account to determine the centrifugal equator. Details of this new diffusive equilibrium density model are given in the appendix.

For simplicity, because the wave frequencies of interest are well above the ion gyrofrequency and the whistler propagation characteristics are primarily controlled by electron density, only two ion species, H^+ and O^+, are included in this analysis. Heavy ions with a complex composition (O^+,O^{2+},S^+,S^{2+}, etc.) dominate near the equator [*Bagenal*, 1994] and the modeled O^+ concentration is adjusted to simulate the effect of all heavy ion species on the plasma scale height at low latitude. H^+ ions must also be included since they become the dominant ion at latitudes above 25° [*Mei et al.*, 1995]. The latitudinal variation of electron density for the adopted (H^+, O^+) model is in excellent agreement (within $\leq$10%) with results obtained for a more realistic multi-ion composition over the important latitude range below 20° where most whistler dispersion occurs. The dispersion is insensitive to the density at higher latitudes ($\sim$ 40°) where the two-ion model differs most from the multi-ion model since the electron density is two orders of magnitude below those at the equator. Electron density contours for the composite model are exhibited in Figure 1. The top panel at λ_{III} = 200° corresponds to the Voyager 1 inbound pass through

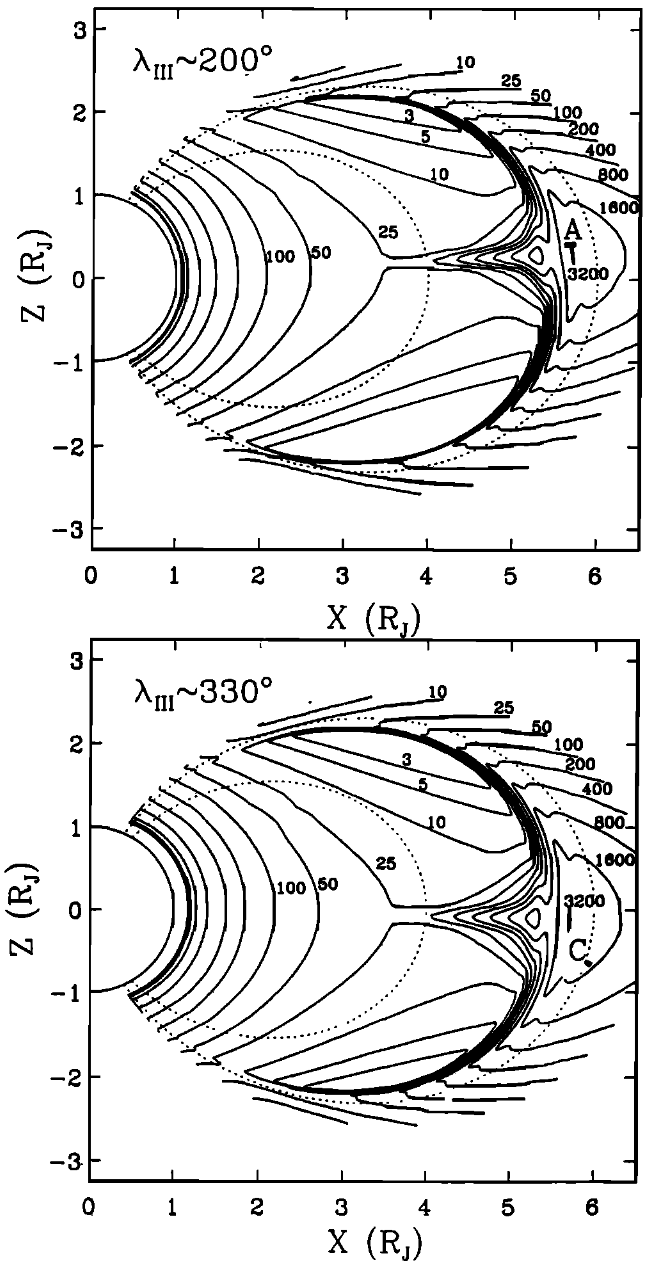

Figure 1. Optimum model electron density contours (per cubic centimeter) in the magnetic meridional plane. The top panel is for λ_{III} = 200°, corresponding to whistler observation in region A. The bottom panel shows density contours for λ_{III} = 330° based on whistler observation in region C. Notice the different positions of the centrifugal equator due to the effect of dipole tilt.

whistler region A ($L \approx 5.7$) when the spacecraft was just above the centrifugal equator. The bottom panel at λ_{III} = 330° corresponds to region C ($L \approx 5.9$) on the outbound pass when Voyager was south of the centrifugal equator.

The ray tracing methodology adopted to analyze whistler dispersion is illustrated in Figures 2 and 3. A basic assumption is that all whistlers are unducted and that the waves are guided from the ionospheric source location to the equatorial observation point (region A or C) by the natural density distribution along the ray path. Backward ray tracing with the HOTRAY code [*Horne*, 1989] is performed through the model environment to identify the source location in the ionosphere. For each observed whistler signal, waves are traced back to the ionosphere, and output from the HOTRAY code is used to plot the resulting time-frequency spectrogram. Key model parameters such as the equatorial ion temperature anisotropy, the equatorial proton concentration, and the equatorial electron density are adjusted until the computed spectrogram agrees with that ob-

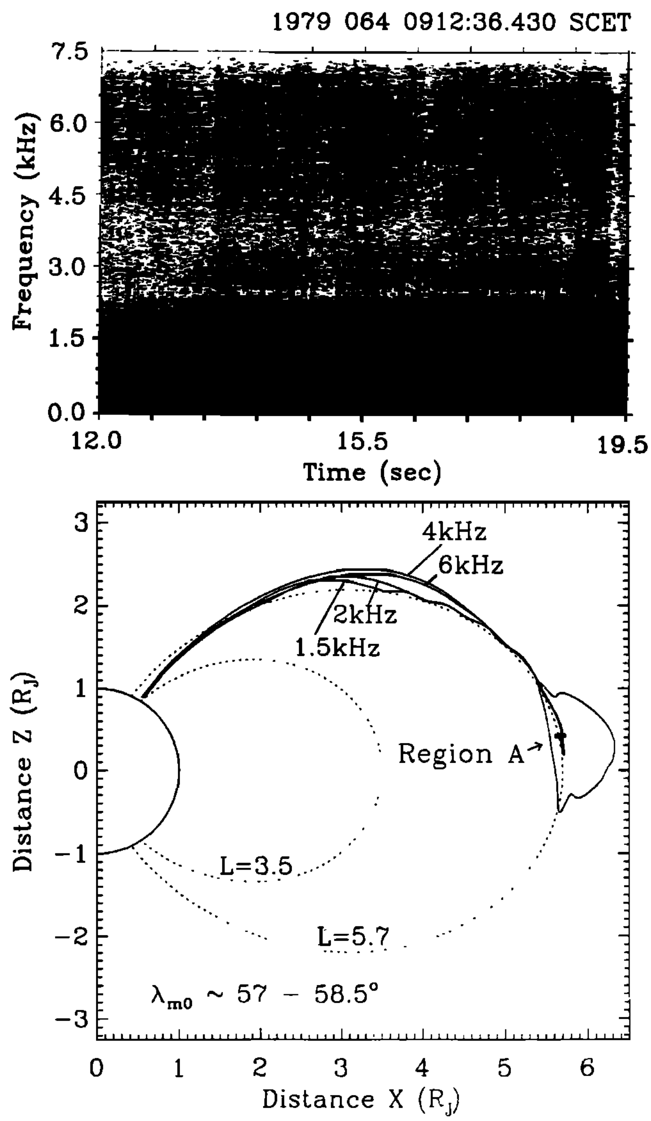

Figure 2. (top) An example of the frequency-time spectrogram for whistlers observed in region A. The dispersion of this signal is 259 s $Hz^{1/2}$ over the observed frequency range from 1.5 kHz to 6 kHz. (bottom) Ray paths of unducted waves originating from Jupiter which have access to region A. Electron density contours near region A and L-shells for $L = 3.5$ (near the ionospheric source point) and $L = 5.7$ are also indicated.

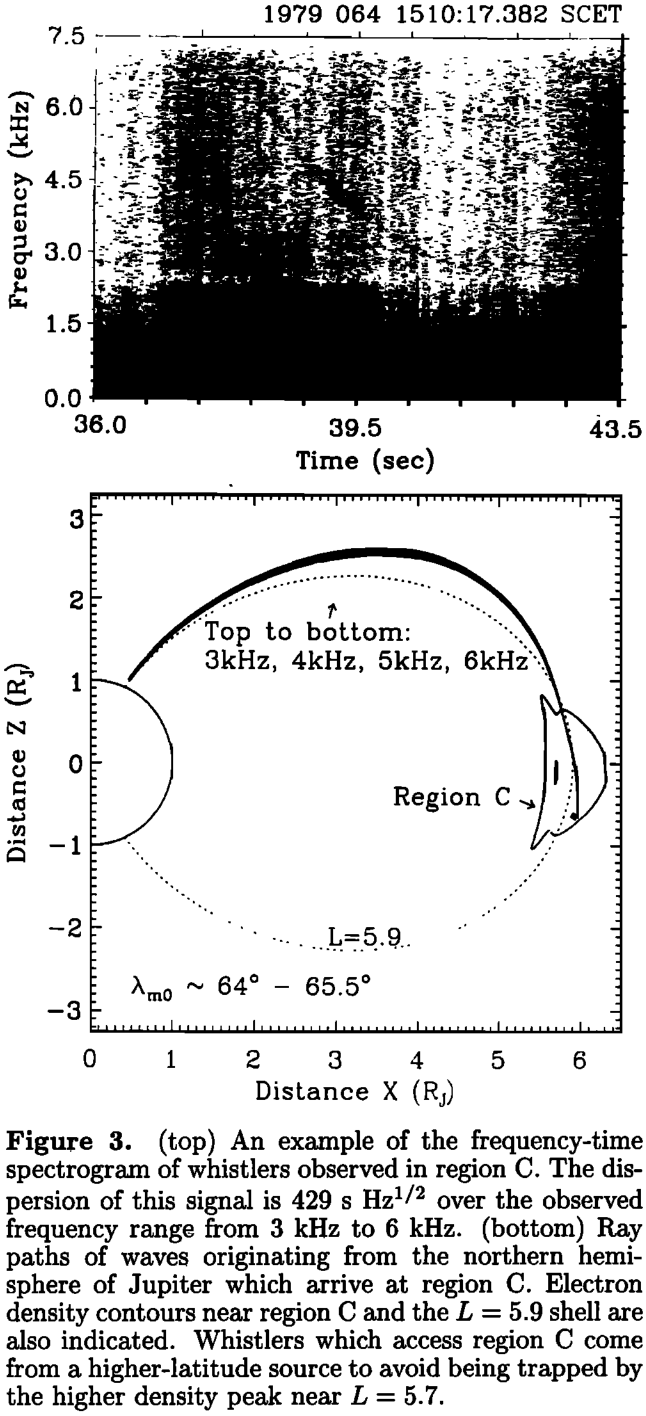

Figure 3. (top) An example of the frequency-time spectrogram of whistlers observed in region C. The dispersion of this signal is 429 s $Hz^{1/2}$ over the observed frequency range from 3 kHz to 6 kHz. (bottom) Ray paths of waves originating from the northern hemisphere of Jupiter which arrive at region C. Electron density contours near region C and the $L = 5.9$ shell are also indicated. Whistlers which access region C come from a higher-latitude source to avoid being trapped by the higher density peak near $L = 5.7$.

served on Voyager. This analysis allows specification of optimum values of important plasma parameters which were not well constrained by direct Voyager observations with the PLS instrument.

3. Results

Five distinct whistlers were observed in region A [*Kurth et al.,* 1985], each with dispersion around 275 s $Hz^{1/2}$ over a frequency range from 1.5 to 6 kHz (e.g., Figure 2, top panel). On the basis of the optimum density model, the source latitudes for all region A whistlers are near 46° Jovigraphic latitude. Six whistlers were observed in region C, with larger dispersion around 420 s $Hz^{1/2}$ and a frequency range from 3 to 6 kHz. Figure 3 (top panel) shows an example of the frequency-time spectrogram for whistlers observed in region C. Backward ray tracing indicates that region C whistlers originate near 64° Jovimagnetic latitude, which at this location corresponds to 61° Jovigraphic latitude. Whistlers which access region A are strongly guided by the dominant density peak at $L = 5.7$. However, for a northern hemisphere source, whistlers which propagate to region C need to come from higher latitudes to avoid being trapped by the higher density peak near $L = 5.7$.

Tables 1 and 2 summarize the optimum parameters for the proton concentration, parallel ion temperature, and the peak density of electrons at the centrifugal equator required to best interpret observed whistler dispersion in both regions A and C. Owing to the restricted spatial distribution of whistler events in regions A and C, only the average dispersions are listed for each region. If all plasma species are assumed to be isotropic ($T_\perp = T_\parallel$) , unreasonably low equatorial electron density would be required to fit the observed dispersion in region A (e.g., in Table 1 for an equatorial proton concentration of 10%, one requires $N_{e0} \sim 2620$ cm^{-3}). Since Voyager 1 directly observed electron density near $N_{e0} = 3250$ cm^{-3} in this region, it is more reasonable to constrain the equatorial electron density to the model values given by *Bagenal* [1994] and fit observed dispersion by allowing the ion temperature anisotropy $A = T_\perp/T_\parallel - 1$ to vary. Temperature anisotropies for heavy ions are expected since the ions sputtered from the Io are preferentially heated in the perpendicular direction by the pickup processes. However, the ionosphere may provide a source of protons, and such ions could be colder and more isotropic. Two extreme models for the proton anisotropy are adopted: $A_{H^+} = 0$ and $A_{H^+} = A_{O^+}$. The results of this fitting procedure are shown in Table 2. The nominal measured perpendicular temperature for O^+ in region A is 40 eV. For a 10% isotropic proton concentration, the parallel temperature of O^+ would have to be 29 eV to best fit the measured whistler dispersion. Alternatively, if both ion

Table 1. Optimum Plasma Parameters Required for an Isotropic Ion Distribution

	Region A			Region C		
Optimum	$L \approx 5.7$, $\bar{D} = 253$			$L \approx 5.9$, $\bar{D} = 420$		
Parameters	$T_{\perp O^+} = 40$ eV, $T_{\perp H^+} = 5$ eV			$T_{\perp O^+} = 60$ eV, $T_{\perp H^+} = 6$ eV		
η_{H^+}, %	10	5	1	10	5	1
N_{e0}, cm^{-3}	2620	2800	3000	2200	2750	3160

Table 2. Optimum Plasma Parameters Required for Anisotropic Ions

Optimum	Region A			Region C		
	$N_{e0} = 3250$			$N_{e0} = 2350$		
Parameters	$T_{\perp O^+} = 40$ eV, $T_{\perp H^+} = 5$ eV			$T_{\perp O^+} = 60$ eV, $T_{\perp H^+} = 6$ eV		
η_{H^+}, %	10	5	1	10	5	1
$A_{H^+} = 0$						
$T_{\parallel O^+}$, eV	29	35	38	56.6	N/A	N/A
$A_{H^+} = A_{O^+}$						
$T_{\parallel O^+}$, eV	33	36	38	57.1	N/A	N/A

species had the same anisotropy $A_{H^+} = A_{O^+}$, the required parallel oxygen temperatures would be 33 eV. As the proton concentration decreases, the required O^+ anisotropy also decreases. For all cases considered, the optimum ion anisotropies required to match observed whistler dispersion lie in a reasonable range between 0 and 1. Whistlers which arrive in region C from a higher-latitude source in the Jovian ionosphere (Figure 3) propagate through regions at intermediate latitude where the density is lower than that corresponding to the $L = 5.7$ density peak. Consequently, the observed dispersion can be fit with the nominal equatorial electron density ($N_{e0} = 2350$ cm^{-3}) obtained from Voyager [*Bagenal*, 1994], even with an essentially isotropic O^+ distribution ($T_{\parallel O^+}$= 56.6 eV). However, in region C the proton concentrations must be close to 10% to yield the observed dispersion (Table 2).

If the lightning source were in the southern hemisphere, waves would need to propagate across the centrifugal equator to reach region A, requiring either much lower equatorial electron density or higher ion temperature anisotropy. In either case the associated minimum plasma density at intermediate latitude would be too low to allow 6-kHz whistlers access to the torus in region A. Even with the more conservative optimum equatorial parameters for region A mentioned above (5% of H^+ and $T_{\parallel O^+} = 35$ eV), 6-kHz whistlers which originate from the southern hemisphere (Figure 4) are strongly refracted at intermediate latitude, due to their oblique propagation through the density minima (~6 cm^{-3}). Consequently, such high-frequency whistlers would be unable to reach region A from a southern latitude source location. The southern hemisphere cannot be the source of region C whistlers, since unreasonably high equatorial electron densities would be required. Consequently, both region A and region C whistlers must originate from lightning activity in the northern hemisphere.

The density minima at intermediate latitudes also provides an important constraint on the maximum frequency for whistlers that reach region A from a northern hemisphere source. Ray paths for 10-kHz whistlers using the optimum model for warm torus are shown in Figure 5. Waves launched from $\lambda_{m0} \leq 59.3°$ are refracted into the inner plasmasphere, whereas waves launched from $\lambda_{m0} \geq 59.4°$ propagate into the outer warm torus where they are subject to severe Landau damping [*Wang et al.*, 1995]. Ten-kilohertz whistlers are consequently unable to reach region A, consistent with Voyager 1 data.

4. Discussion and Conclusions

A new 3-D model for the plasma distribution in the inner Jovian magnetosphere has been developed using an offset and tilted dipole magnetic field. This analytical density model has been used in the HOTRAY code to follow the ray path of unducted lightning-generated whistlers from source locations in the Jovian ionosphere to the equatorial observation location along the Voyager 1 trajectory. Model parameters such as the H^+ composition, the ion temperature anisotropy, and the equatorial electron density have been optimized to best simulate the observed dispersion and frequency range of whistlers in the warm Io torus.

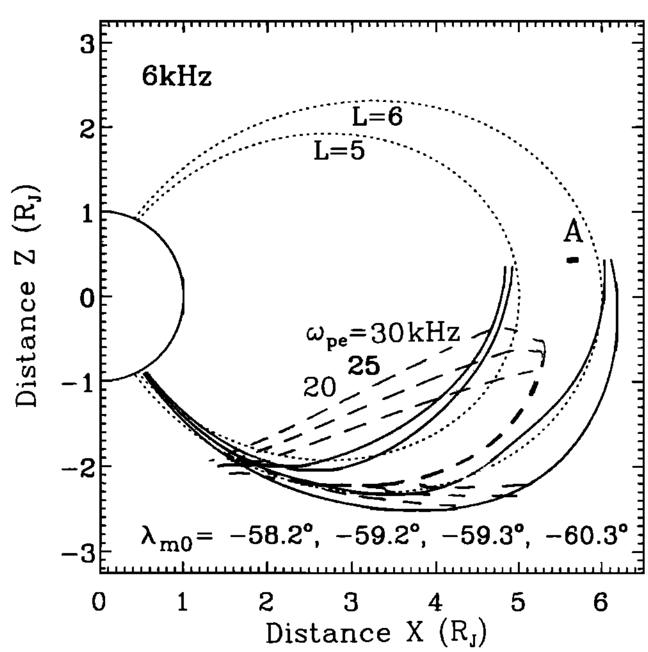

Figure 4. Six-kilohertz waves launched from the southern hemisphere cannot gain access to region A due to lower plasma density in the southern hemisphere (due to the dipole tilt) in our optimum density model (Table 1). The dashed lines show contours of plasma frequency.

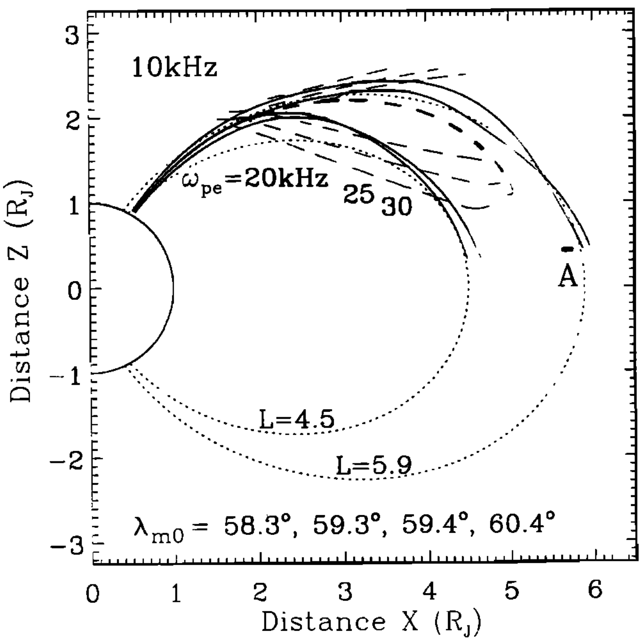

Figure 5. Ten-kilohertz waves are unable to access region A from a source location in the northern hemisphere due due to the low plasma density at high latitudes in our optimum density model. Waves launched from latitudes lower than 59.3° propagate to the inner plasmasphere around $L = 4.5$, and waves launched from latitude higher than 59.4° propagate to the outer region beyond region A around $L = 5.9$.

Modest thermal ion temperatures anisotropy ($T_{\|} \ll T_{\perp}$) is required to account for the dispersion of whistlers seen near $L = 5.7$ during the inbound Voyager 1 pass through the warm torus (region A), consistent with the previous dispersion analysis by *Crary et al.* [1996] in which field-aligned (ducted) propagation was assumed. Whistler dispersion observed near $L = 5.9$ on the outbound trajectory (region C) requires substantial ($\geq$10%) H^+ concentration. There is a tendency toward higher H^+ concentration with increasing L-shell, as noted in earlier studies [*Tokar et al.*, 1982a, b; *Crary et al.*, 1996]. The optimum plasma parameters required to best fit observed wave dispersion also yield a deep density minimum at intermediate latitudes, which provides a natural upper cutoff to the whistler spectrum, consistent with Voyager observations.

The source locations in the Jovian ionosphere for region A and C whistlers are around $\Lambda_g = 45°$ to 60° in the northern hemisphere. This is much lower than that suggested in previous studies by *Menietti and Gurnett* [1980] and *Hobara et al.* [1995]. The source latitudes predicted in our model correspond approximately to where optical lightning events were observed by Voyager 1 [*Cook et al.*, 1979; *Magalhães and Borucki*, 1991]. Furthermore, all the optical lightning events were confined to the northern hemisphere, consistent with this ray tracing simulation. Higher-order terms of magnetic field could modify the precise source location in the Jovian ionosphere, but the effect is not expected to be large.

Appendix: Density Model

All plasma species are assumed to be bi-Maxwellian in diffusive equilibrium along field lines under the balance between magnetic, gravity, and centrifugal force. The latitudinal variation of temperature anisotropy is also considered [*Huang and Birmingham*, 1992]. Assuming that the parallel temperature along field lines does not change, the density of each species can be written as:

$$\frac{n_{e,c}}{n_{e,c0}} = \frac{T_{e\perp}}{T_{e0\perp}}\exp[\frac{e}{T_{e\|}}(\Phi_E - \Phi_{E,0})] \quad (1)$$

$$\frac{n_{e,h}}{n_{e,h0}} = \frac{T_{h\perp}}{T_{h0\perp}}\exp[\frac{e}{T_{h\|}}(\Phi_E - \Phi_{E,0})] \quad (2)$$

$$\frac{n_{\alpha}}{n_{\alpha,0}} = \frac{T_{\alpha\perp}}{T_{\alpha0\perp}}\exp[\Phi_\alpha - \frac{Z_\alpha e}{T_{\alpha\|}}(\Phi_E - \Phi_{E,0})] \quad (3)$$

Here $n_{e,c}$, $n_{e,h}$, n_α denote density for cold electron, suprathermal electron, and ion species α, and Φ_α is the sum of the gravitational and centrifugal potential for each ion species α.

$$\Phi_\alpha = -\frac{m_\alpha}{T_{\alpha\|}}GM_J(\frac{1}{r} - \frac{1}{r_0}) + \frac{1}{2}\frac{m_\alpha}{T_{\alpha\|}}\Omega_J^2(\rho^2 - \rho_0^2) \quad (4)$$

and,

$$\frac{T_{\alpha\perp}}{T_{\alpha0\perp}} = [1 + A_\alpha(1 - \frac{B_0}{B})]^{-1} \quad (5)$$

where $A_\alpha \equiv T_{\alpha0\perp}/T_{\alpha0\|} - 1$. The subscript 0 refers to the reference point along a field line (usually the centrifugal equator); ρ, r, and B represent distance to the rotational axis, the radial distance, and magnetic field strength at any other location along the field line.

The offset and tilt of the dipole magnetic field are considered to determine the position of the centrifugal equator which occurs where the distance to the rotational axis is largest. Figure 6 shows the case when the center of dipole D is offset from the Jovigraphic center J by a distance Δ along System III longitude μ at a

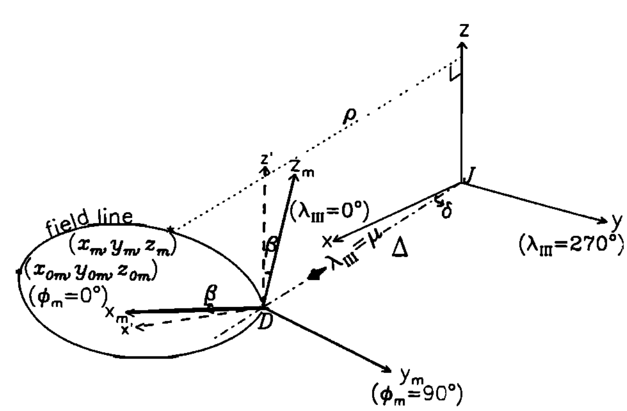

Figure 6. Transformation from Jovigraphic coordinates x, y, z to Jovimagnetic coordinates x_m, y_m, z_m: (1) Offset by $\Delta(R_J)$, z axis moves to z'. (2) Tilt by $\beta°$, z' axis rotates to z_m. Here ρ is the radial distance from a point along any field line to the rotational axis z. Note that after transformation, the dipole is tilting toward $\phi_m = 180°$

latitude δ for the OTD parameters taken from *Acuña et al.* [1983]. The dipole axis is further tilted by an angle β pointed to System III longitude Φ_β. The term in (4) for the change in centrifugal potential $\rho^2 - \rho_0^2$ can then be described in magnetic coordinates since

$$\begin{aligned}\rho^2 - \rho_0^2 = &(\cos\beta\, x_m + \sin\beta\, z_m)^2 \\ &-(\cos\beta\, x_{0m} + \sin\beta\, z_{0m})^2 + y_m^2 - y_{0m}^2 \\ &+2\Delta\cos\delta \times [(\sin\mu\cos(\Phi_\beta - \mu) \\ &-\cos\mu\sin(\Phi_\beta - \mu))(y_m - y_{0m}) \\ &+(\cos\mu\cos(\Phi_\beta - \mu) \\ &+\sin\mu\sin(\Phi_\beta - \mu))(\cos\beta\,(x_m - x_{0m}) \\ &- \sin\beta\,(z_m - z_{0m})] \qquad (6)\end{aligned}$$

From (1) - (3), the density of both suprathermal electrons and ions can be expressed in terms of the density of cold electrons.

$$\frac{n_{e,h}}{n_{e,h0}} = \frac{T_{h\perp}}{T_{h0\perp}}\left[\frac{n_{e,c}}{n_{e,c0}}\frac{T_{e0\perp}}{T_{e\perp}}\right]^{\frac{T_{e\parallel}}{T_{h\parallel}}} \qquad (7)$$

$$\frac{n_\alpha}{n_{\alpha,0}} = \frac{T_{\alpha\perp}}{T_{\alpha0\perp}}\exp[\Phi_\alpha]\left[\frac{n_{e,c}}{n_{e,c0}}\frac{T_{e0\perp}}{T_{e\perp}}\right]^{-Z_\alpha\frac{T_{e\parallel}}{T_{\alpha\parallel}}} \qquad (8)$$

Charge neutrality requires

$$\begin{aligned}&\frac{n_{e,c}}{n_{e,c0}} + \frac{n_{e,h0}}{n_{e,c0}}\left[\frac{n_{e,c}}{n_{e,c0}}\frac{T_{e0\perp}}{T_{e\perp}}\right]^{\frac{T_{e\parallel}}{T_{h\parallel}}}\left(\frac{T_{h\perp}}{T_{h0\perp}}\right) \\ &= \sum_\alpha Z_\alpha \frac{n_{\alpha,0}}{n_{e,c0}}\frac{T_{\perp,\alpha}}{T_{\perp,\alpha0}}\exp[\Phi_\alpha]\left[\frac{n_{e,c}}{n_{e,c0}}\frac{T_{e0\perp}}{T_{e\perp}}\right]^{-Z_\alpha\frac{T_{e\parallel}}{T_{\alpha\parallel}}} \qquad (9)\end{aligned}$$

Since it is reasonable to assume that electrons are isotropic everywhere, (9) can be simplified to

$$\begin{aligned}&\frac{n_{e,c}}{n_{e,c0}} + \frac{n_{e,h0}}{n_{e,c0}}\left[\frac{n_{e,c}}{n_{e,c0}}\right]^{\frac{T_{e\parallel}}{T_{h\parallel}}} \\ &= \sum_\alpha Z_\alpha \frac{n_{\alpha,0}}{n_{e,c0}}\frac{T_{\alpha\perp}}{T_{\alpha0\perp}} exp[\Phi_\alpha]\left[\frac{n_{e,c}}{n_{e,c0}}\right]^{-Z_\alpha\frac{T_{e\parallel}}{T_{\alpha\parallel}}} \qquad (10)\end{aligned}$$

The suprathermal electron term can usually be ignored since the fractional composition is less than a few percent inside $L = 10$. Furthermore, in the torus where $T_{e\parallel} \ll T_{\alpha\parallel}/Z_\alpha$, we may follow *Mei et al.* [1995] and obtain an approximate analytical solution:

$$\frac{n_{e,c}}{n_{e,c0}} \approx \left(\sum_\alpha Z_\alpha \frac{n_{\alpha,0}}{n_{e,c0}}\frac{T_{\alpha\perp}}{T_{\alpha0\perp}}\exp[\Phi_\alpha]\right)^{\frac{1}{1+Z_\alpha\frac{T_{e\parallel}}{T_{\alpha\parallel}}}} \qquad (11)$$

Acknowledgments. The authors thank F. Bagenal and K. Khurana for valuable discussions concerning the OTD model. Also thanks to J. B. Groene of the University of Iowa for assistance in processing Voyager 1 data. Voyager 1 data are provided by the Outer Planets Subnode of the Planetary Plasma Interactions Node of the Planetary Data System. Computational resources were provided by the San Diego Supercomputing Center. This work was supported by NASA grant NAG5-6265 and NSF grant ATM97 29021.

The Editor thanks Michael L. Kaiser and another referee for their assistance in evaulating this paper.

References

Acuña, M. H., K. W. Behannon, and J. E. P. Connerney, Jupiter's magnetic field and magnetosphere, in *Physics of the Jovian Magnetosphere*, edited by A. J. Dessler, pp. 1-50, Cambridge Univ. Press, New York, 1983.

Bagenal, F., R. L. McNutt Jr., J. W. Belcher, H. S. Bridge, and J. D. Sullivan, Revised ion temperatures for Voyager plasma measurements in the Io plasma torus, *J. Geophys. Res.*, *90*, 1755, 1985.

Bagenal, F., Empirical model of the Io plasma torus: Voyager 1 measurements, *J. Geophys. Res.*, *99*, 11,043, 1994.

Cook, A.F., T. C. Duxbury, and G. E. Hunt, First results on Jovian lightning, *Nature*, *280*, 794, 1979.

Crary, F. J., F. Bagenal, J. A. Ansher, D. A. Gurnett, and W. S. Kurth, Proton density and thermal anisotropy of the Io plasma torus derived from whistler wave dispersion, *J. Geophys. Res.*, *101*, 2699, 1996.

Divine, N., and H. B. Garrett, Charged particle distributions in Jupiter's magnetosphere, *J. Geophys. Res.*, *88*, 6889, 1983.

Frank, L. A., K. L. Ackerson, J. H. Wolfe, and J. D. Mihalov, Observations of plasma in the Jovian magnetosphere, *J. Geophys. Res.*, *81*, 457, 1976.

Gurnett, D. A., and F. L. Scarf, Plasma waves in the Jovian magnetosphere, in *Physics of the Jovian Magnetosphere*, edited by A. J. Dessler, pp. 285-316, Cambridge University Press, New York, 1983.

Gurnett, D. A., P. R. Shaw, R. R. Anderson, and W. S. Kurth, Whistlers observed by Voyager 1: Detection of lightning on Jupiter, *Geophys. Res. Lett.*, *6*, 511, 1979.

Gurnett, D. A., F. L. Scarf, W. S. Kurth, R. R. Shaw, and R. L. Poynter, Determination of Jupiter's electron density profile from plasma wave observations, *J. Geophys. Res.*, *86*, 8199, 1981.

Helliwell, R. A., *Whistlers and Related Ionospheric Phenomena*, Stanford Univ. Press, Stanford, Calif., 1965.

Hobara, Y., O. A. Molchanov, M. Hayakawa, and K. Ohta, Propagation characteristics of whistler waves in the Jovian ionosphere and magnetosphere, *J. Geophys. Res.*, *100*, 23,523, 1995.

Horne, R. B., Path-integrated growth of electrostatic waves: The generation of terrestrial myriametric radiation, *J. Geophys. Res.*, *94*, 8895, 1989.

Huang, T. S., and T. J. Birmingham, The polarization electric field and its effects in an anisotropic rotating magnetospheric plasma, *J. Geophys. Res.*, *97*, 1511, 1992.

Kurth, W. S., B. D. Strayer, D. A. Gurnett, and F. L. Scarf, A summary of whistlers observed by Voyager 1 at Jupiter, *Icarus*, *61*, 497, 1985.

Magalhães, L. A., and W. J. Borucki, Spatial distribution of visible lightning on Jupiter, *Nature*, *349*, 311, 1991.

Mei, Y., R. M. Thorne, and F. Bagenal, Analytical model for the density distribution in the Io plasma torus, *J. Geophys. Res.*, *100*, 1823, 1995.

Menietti, J. D., and D. A. Gurnett, Whistler propagation in the Jovian magnetosphere, *Geophys. Res. Lett.*, *7*, 49, 1980.

Sentman, D. D., and C. K. Goertz, Whistler mode noise in Jupiter's inner magnetosphere, *J. Geophys. Res.*, *83*, 3152, 1978.

Smith, R. L., and J. J. Angerami, Magnetospheric properties deduced from OGO 1 observations of ducted and non-ducted whistlers, *J. Geophys. Res.*, *73*, 1, 1968.

Strobel, D. F., and S. K. Atreya, Ionosphere, in *Physics of the Jovian Magnetosphere*, edited by A. J. Dessler, pp. 51-67, Cambridge Univ. Press, New York, 1983.

Tokar, R. L., D. A. Gurnett, F. Bagenal, and R. R. Shaw, Light ion concentrations in Jupiter's inner magnetosphere, *J. Geophys. Res.*, *87*, 2241, 1982a.

Tokar, R. L., D. A. Gurnett, and F. Bagenal, The proton concentration in the vicinity of the Io plasma torus, *J. Geophys. Res., 87,* 10,395, 1982b.

Wang, K., R. M. Thorne, and R. B. Horne, The propagation characteristics and Landau damping of Jovian whistlers in the Io torus, *J. Geophys. Res., 100,* 21,709, 1995.

Wang, K., R. M. Thorne, R. B. Horne, and W. S. Kurth, Cold torus whistlers: An indirect probe of the inner Jovian plasmasphere, *J. Geophys. Res.,* this issue.

R. B. Horne, British Antarctic Survey, Madingley Road, Cambridge, CB3 OET, England. (e-mail: R.Horne@bas.ac.uk)

W. S. Kurth, Department of Physics and Astronomy, University of Iowa, Iowa City, IA 52242-1479. (e-mail: william-kurth@uiowa.edu)

R. M. Thorne, Department of Atmospheric Sciences, University of California at Los Angeles, CA 90095-1565. (e-mail: rmt@jupiter.atmos.ucla.edu)

K. Wang, M/S 169-506, Jet Propulsion Laboratory, 4800 Oak Grove Drive, Pasadena, CA, 91109-8099. (e-mail: kwang@jplsp.jpl.nasa.gov)

(Received September 22, 1997; revised March 2, 1998; accepted March 16, 1998.)